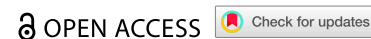



ORIGINAL RESEARCH



## Loss of the extracellular protease ADAMTS1 reveals an antitumorigenic program involving the action of NIDOGEN-1 on macrophage polarization

Rita Caracuel-Peramos<sup>a</sup>, Francisco Javier Rodríguez-Baena<sup>a†</sup>, Silvia Redondo-García<sup>a‡</sup>, Juan Antonio Villatoro-García<sup>a,b</sup>, Ana García-Muñoz<sup>a</sup>, Carlos Peris-Torres<sup>a</sup>, María del Carmen Plaza-Calonge<sup>a</sup>, Alba Rubio-Gayarre<sup>a</sup>, Belén López-Millán<sup>a,c</sup>, Carmela Ricciardelli<sup>d</sup>, Darryl L. Russell<sup>e</sup>, Pedro Carmona-Sáez<sup>a,b</sup>, and Juan Carlos Rodríguez-Manzanque<sup>a</sup> 

<sup>a</sup>GENYO. Centre for Genomics and Oncological Research: Pfizer/Universidad de Granada/Junta de Andalucía, Granada, Spain; <sup>b</sup>Department of Statistics, University of Granada, Granada, Spain; <sup>c</sup>Department of Physiology, University of Granada, Granada, Spain; <sup>d</sup>Robinson Research Institute, Adelaide Medical School, University of Adelaide, Adelaide, Australia; <sup>e</sup>Robinson Research Institute, School of Biomedicine, University of Adelaide, Adelaide, Australia

### ABSTRACT

Recent research highlighted the contribution of extracellular matrix, and particularly of ADAMTS proteases, in immune regulation. Now, our work with melanoma and mammary tumor models revealed that tumor blockade induced by the lack of *Adamts1* led to an increased vascular deposition of its substrate, the basement membrane glycoprotein NIDOGEN-1 (NID1). Significantly, the overexpression of NID1 in the melanoma syngeneic model also blocked tumor progression, disclosing an overlapping phenotype with the absence of *Adamts1*. These tumors showed important alterations in their immune infiltrates, emphasizing an enhanced presence of antitumorigenic macrophages and a global inflammatory landscape. We corroborated *in vitro* that full length NID1, but not its fragments, promoted an M1-like macrophage polarization, mainly mediated by the  $\alpha\beta3$  integrin. Significantly, the projection of RNA-seq from our tumor models to two large human melanoma datasets allowed us to discover a new gene signature associated with good prognosis and the abundance of M1-like macrophages. These results support NID1 as a novel tumor suppressor with immunomodulatory properties, and unveil the existence of key oncological drivers in the extracellular scenario.

### ARTICLE HISTORY

Received 4 October 2024  
Revised 12 April 2025  
Accepted 15 May 2025

### KEYWORDS

Bioinformatics; extracellular matrix; macrophages; melanoma immune infiltration; syngeneic mouse model

### Introduction

In recent decades, cancer has increasingly been recognized as a complex ecosystem, where diverse cellular entities interact within a dynamic extracellular matrix (ECM). Notably, ECM deregulation can promote both pro- and antitumorigenic pathways.<sup>1</sup> The proteolysis of ECM by matrix-degrading enzymes continues to uncover the vast regulatory potential of this intricate network, influencing a wide range of biological processes.<sup>2,3</sup>

For years, the ADAMTS (*A Disintegrin And Metalloprotease with ThromboSpondin repeats*) protease family has been related with angiogenesis and carcinogenesis.<sup>4,5</sup> Recently, we found that ADAMTS1 also plays a role in regulating the immune response in both healthy and tumor-bearing mice.<sup>6</sup> While the catalytic activity of this protease on various proteoglycans and other extracellular components has already been reported, studies correlating biological actions and substrates remain limited. Using two immunocompetent mouse tumor models, we now reveal that the absence of *Adamts1* correlates with changes in the glycoprotein Nidogen-1 (NID1), one of its relevant substrates.<sup>7</sup> NID1, primarily reported as a basement membrane (BM) component, regulates adhesion, migration

and invasion,<sup>8</sup> but no biological functions have yet been attributed to its proteolyzed forms.


Within the complex tumor immune microenvironment, tumor-associated macrophages (TAMs) have emerged as important prognostic factors across various cancers.<sup>9,10</sup> These cells exist along a dynamic spectrum of subpopulations and identities, reflecting their molecular and functional diversity. While emerging research is refining classification beyond the traditional paradigm,<sup>9,11</sup> the distinction between classically activated (M1-like) macrophages -which support inflammation and are associated with better clinical outcomes- and alternatively activated (M2-like) -which suppress antitumor immunity- remains a useful framework for understanding macrophage functionality.<sup>12</sup> The influence of soluble factors on TAM behavior is well documented,<sup>13</sup> however the role of ECM constituents remains less understood. Moreover, targeting ECM-immune cell interactions presents promising new strategies for enhancing immunotherapies, potentially overcoming some of the challenges posed by the tumor microenvironment (TME).

In this study, we demonstrate that NID1 enhances tumor immune infiltration and specifically educates macrophages toward an antitumorigenic state, thereby inhibiting tumor

**CONTACT** Juan Carlos Rodríguez-Manzanque ✉ [juancarlos.rodriguez@genyo.es](mailto:juancarlos.rodriguez@genyo.es) GENYO. Centre for Genomics and Oncological Research: Pfizer/Universidad de Granada/Junta de Andalucía, Avenida de la Ilustración, 114, Granada, 18016 Spain

<sup>†</sup>Present affiliation: Instituto de Neurociencias CSIC-UMH, San Juan de Alicante, 03550 Spain.

<sup>‡</sup>Present affiliation: Centre for Cancer Immunology, Faculty of Medicine, University of Southampton, Southampton, UK.

 Supplemental data for this article can be accessed online at <https://doi.org/10.1080/2162402X.2025.2508057>

© 2025 The Author(s). Published with license by Taylor & Francis Group, LLC.

This is an Open Access article distributed under the terms of the Creative Commons Attribution-NonCommercial License (<http://creativecommons.org/licenses/by-nc/4.0/>), which permits unrestricted non-commercial use, distribution, and reproduction in any medium, provided the original work is properly cited. The terms on which this article has been published allow the posting of the Accepted Manuscript in a repository by the author(s) or with their consent.

progression. By integrating transcriptomic data from our murine melanoma models with human melanoma cohorts, we identified a gene signature associated with M1-like macrophage abundance, which correlates with improved patient outcomes. Notably, our tumor models offer new insights into the impact of ECM modification, shedding light on the ADAMTS1/NID1 relationship and underscoring the importance of assessing ECM proteolysis in specific tumor contexts.

## Materials and methods

See Supplementary Information.

## Results

### Vascular deposition of NID1 increases in the absence of *Adamts1* and correlates with reduced tumor progression

To explore cancer-related pathways modulated by ADAMTS1, we assessed two mouse tumor models: the syngeneic B16F1 melanoma<sup>14</sup> and the spontaneous MMTV-PyMT mammary tumor,<sup>15</sup> using WT and *Adamts1*-knockout (Ats1-KO) mice (Figure 1a). As published, tumor growth is significantly delayed in Ats1-KO mice in both models.<sup>14,15</sup> While previous studies revealed altered vascular parameters in the B16F1 model lacking stromal *Adamts1*,<sup>14</sup> MMTV-PyMT derived tumors in WT and Ats1-KO mice showed no relevant differences (Supplementary Figure S1A-B).

According to our previous data confirming the action of ADAMTS1 on basement membrane nidogens,<sup>7,16</sup> we evaluated NID1 and NID2 levels in tumor sections of these models. Confocal microscopy showed a significant increase of NID1 deposition around the vasculature in the absence of *Adamts1* (Figure 1b), while no relevant changes were observed for its paralog NID2 (Supplementary Figure S1C).

### Overexpression of NID1 blocks tumor progression

To elucidate the contribution of NID1, we generated B16F1 cells overexpressing it (designated B16Nid1), as parental B16F1 cells lack endogenous *Nid1*. NID1 overexpression was confirmed in B16Nid1 cells and did not affect proliferative capacity (Supplementary Figure S2).

Significantly, NID1 overexpression delayed tumor growth in WT mice (Figure 2a), as corroborated by endpoint tumor weight and volume measurements (Figure 2b). In Ats1-KO mice, B16Nid1 cells did not show synergistic effects compared with WT mice (Supplementary Figure S3A). Histological analysis of B16Nid1 tumors revealed increased NID1 deposition, mostly around vessels (Figure 2c), without major alterations in vascular features (Figure 2d and Supplementary Figure S3B-C). Overall, the B16Nid1 tumor phenotype closely resembled that of parental B16F1 cells in Ats1-KO mice,<sup>14</sup> including tumor growth blockade and increased NID1 staining in the vasculature.

### ***NID1 overexpression is accompanied by an increased tumor immune infiltration, including a relevant population of antitumorigenic macrophages***

Given the phenotypic similarities between the new B16Nid1 model and previously reported B16F1-Ats1KO tumors,<sup>6</sup> we investigated immune infiltration. RNA-seq deconvolution using CIBERSORT<sup>17</sup> confirmed that both tumor types share immune profiles that differ from B16F1 controls (Supplementary Figure S4A). Flow cytometry (FC) analysis further revealed increased infiltration of T cells (CD3+) and myeloid cells (CD11b+) in B16Nid1 tumors compared to B16F1 controls. A detailed examination of the myeloid compartment demonstrated a higher abundance of macrophages (CD11b+ F4/80+), while myeloid-derived suppressor cells (MDSCs, CD11b+ Gr1+) were reduced in *Nid1*-overexpressing tumors (Figure 3a). Dendritic cells (CD11b+ CD11c+) were barely detectable in this model, with no significant differences between groups (Figure 3a).

Given the prominent infiltration of myeloid cells, particularly macrophages, in this tumor model, we characterized this population by isolating CD11b+ cells from each tumor group (Figure 3b) and performing RNA-seq. The transcriptomic profiles of these myeloid cells exhibited distinct patterns depending on tumor origin, revealing a total of 1407 DEGs, with 515 upregulated and 892 downregulated in B16Nid1 samples (Figure 3c).

To assess the biological significance of these transcriptomic changes, we conducted enrichment analyses across different databases. Gene ontology (GO) analysis highlighted significant enrichment in pathways related to adaptive immune activation and responses to interferon-gamma (IFN- $\gamma$ ) and interferon-beta (IFN- $\beta$ ) (Figure 3d). Reactome analysis further identified enrichment in pathways associated with myeloid cell activation and migration (DAP12 signaling), antigen processing (FCGR activation), T-cell activation (CD28 costimulation) and pro-inflammatory cytokine responses (IL12 signaling) (Figure 3e). Collectively, these findings underscore the high plasticity of the myeloid compartment in response to environmental cues, suggesting an activated and immunostimulatory state in B16Nid1 tumors.

Recognizing the heterogeneous and plastic nature of macrophages, we examined their functional polarization within the classical M1/M2 activation framework, which remains widely used in recent literature despite its limitations in capturing the full heterogeneity of TAMs.<sup>12</sup> Transcriptomic profiling of upregulated genes in B16Nid1-derived CD11b+ cells revealed a gene expression pattern more closely aligned with M1-like than M2-like macrophages (Figure 3f). Additionally, gene set enrichment analyses (GSEA) corroborated a positive and significant enrichment of M1-associated genes in CD11b+ cells from B16Nid1 tumors (Figure 3g).

Consistent with the transcriptomic characterization, we assessed TAMs dynamics at protein level using FC for two classical polarization markers: MHC-II (M1-like) and CD206 (M2-like). These analyses revealed a shift toward an M1-like phenotype, with an increased proportion of MHC-II<sup>+</sup> CD206<sup>-</sup> macrophages and a reduction of MHC-II<sup>-</sup> CD206<sup>+</sup> macrophages in B16Nid1 tumors. The

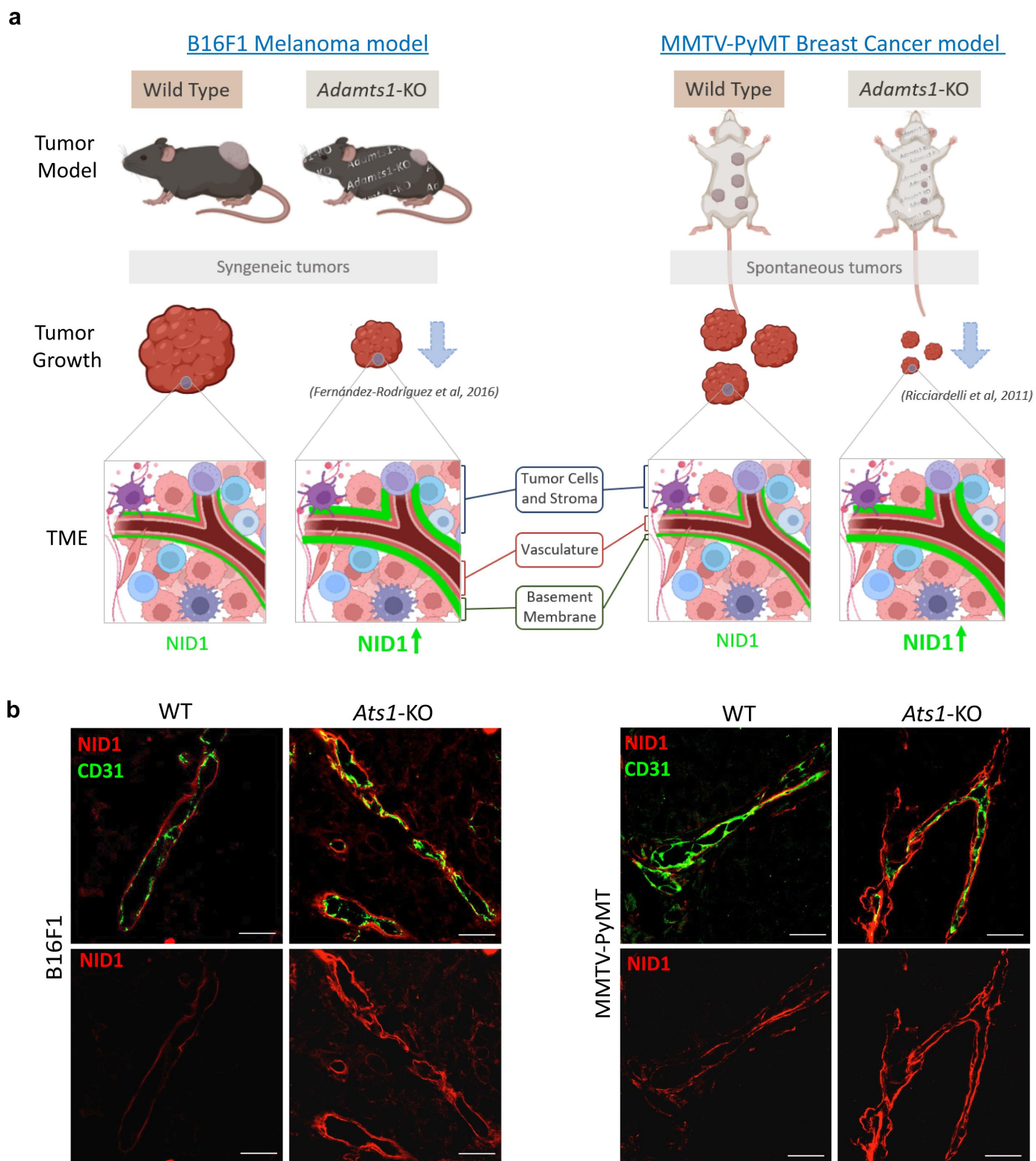


**Figure 1.** Scheme of B16F1 and MMTV-PyMT tumor models and NID1 deposition changes in an ADAMTS1-dependent manner. (a) Schematic representation of B16F1 and MMTV-PyMT models remarking their characteristics and the reported reduction of tumor growth in the absence of ADAMTS1. The illustration highlights main compartments such as: “tumor Cells and stroma”, “vasculature” and “basement membrane”, and the increased deposition of NID1 in *Ats1-KO* mice. (b) Representative images of tumor vasculature showing CD31 (green) and NID1 (red) immunofluorescence co-staining of B16F1 and MMTV-PyMT tumors in WT and *Ats1-KO* mice (merge staining in top and single NID1 in bottom file). White scale bar = 20  $\mu$ m.

intermediate M1-M2 TAM population (MHC-II<sup>+</sup> CD206<sup>+</sup>) remained unchanged between tumor models (Figure 3h). This polarization shift correlated with the inhibition of tumor progression driven by NID1 overexpression.

Finally, cytokine analysis in tumor lysates and serum from tumor-bearing mice revealed variations consistent with an antitumorigenic environment following NID1 overexpression (Supplementary Figure S5).



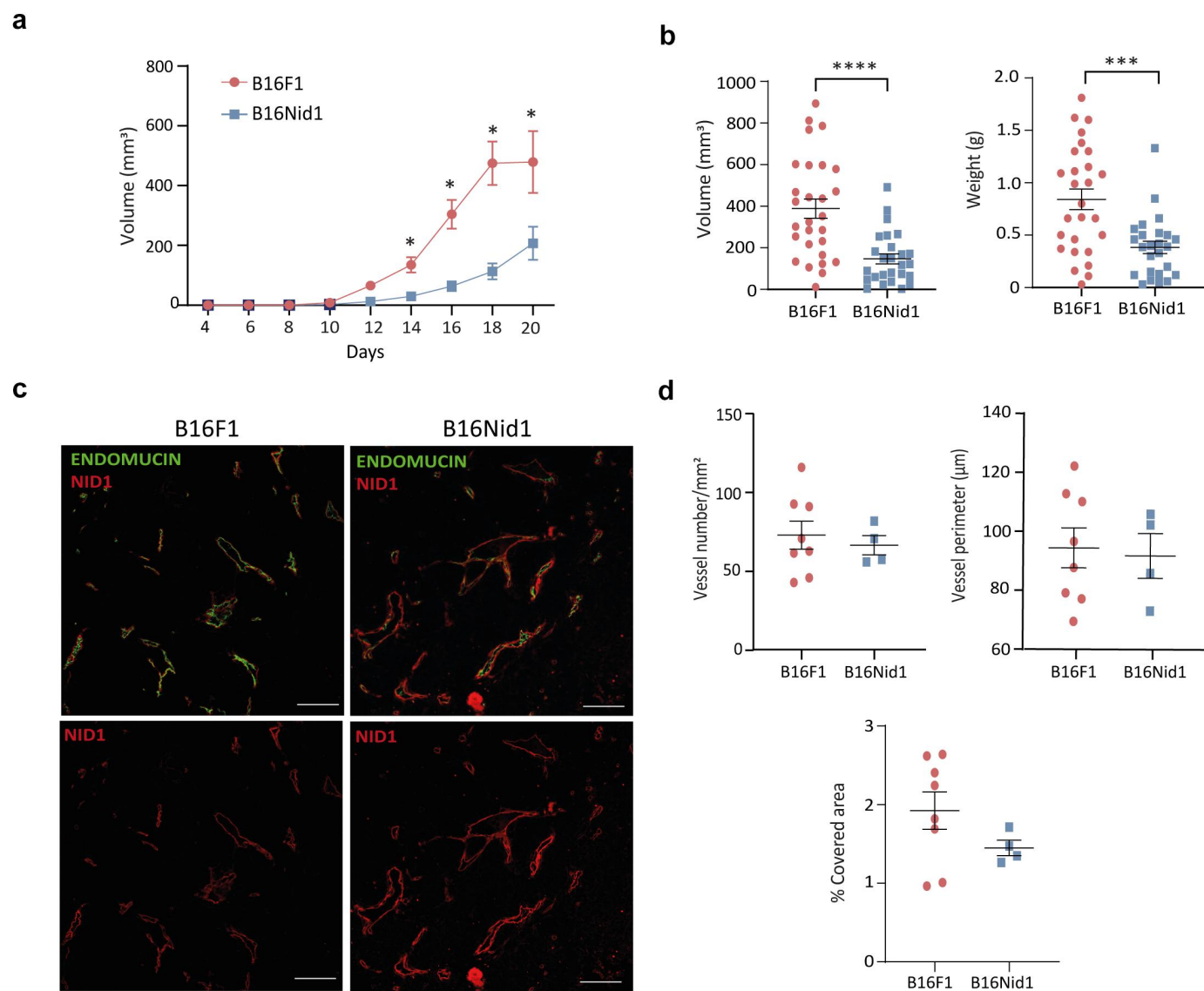


**Figure 2.** Progression and vasculature characterization of tumors generated by control and NID1-overexpressing B16F1 cells. (a) Evolution of the mean tumor volume of B16F1 and B16Nid1 groups ( $n > 20$  per group). (b) Graphs representing volume and weight of B16F1 and B16Nid1 tumors at final point ( $n > 20$  per group). (c) Representative images of tumor vasculature showing ENDOMUCIN (green) and NID1 (red) immunofluorescence co-staining of B16F1 and B16Nid1 tumors (merge staining in top and single NID1 in bottom file). White scale bar = 100 μm. (d) Quantification of tumor vasculature parameters: vessel density, perimeter and percentage of covered area ( $n = 8$  for B16F1,  $n = 4$  for B16Nid1). (\* $p < 0.05$ ; \*\*\* $p < 0.001$ ; \*\*\*\* $p < 0.0001$ ).

### NID1-overexpressing cells educate macrophages toward an M1-like polarization state through $\alpha v \beta 3$ integrin

Given the extracellular and secreted nature of NID1, we performed *in vitro* polarization experiments. Bone marrow-derived macrophages (BMDMs) were treated with conditioned media (CM) from B16F1 or B16Nid1 tumor cells. Notably, qPCR analyses revealed increased expression of several M1-associated markers in BMDMs treated with NID1-containing CM, while the M2 marker *Mrc1* remained unchanged (Figure 4a). This effect was also observed in murine RAW 264.7 (Figure 4b) and human THP-1 macrophage cells (Figure 4c). FC further confirmed M1-like polarization, showing induction of NOS2 and MHC-II, along with reduced CD206 in B16Nid1 CM-treated BMDMs (Figure 4d–e).

To date, few reports have identified a cell receptor for NID1 actions. Among them, the integrin  $\alpha v \beta 3$  (CD51/CD61) has been found in macrophages.<sup>8</sup> To investigate its role, BMDMs

were pre-treated with the  $\alpha v \beta 3$  antagonist cilengitide (HY-16141, MedChemExpress) prior to polarization. This pre-treatment markedly reduced *Nos2* expression induced by NID1-containing CM. Expression of additional M1 markers followed a similar inhibitory trend (Figure 4f). Moreover, we analyzed AKT phosphorylation as a marker of macrophage activation.<sup>18</sup> Indeed, CM from B16Nid1 cells induced AKT phosphorylation, which was prevented by cilengitide pre-treatment (Figure 4g–h), confirming that NID1 polarizes macrophages via  $\alpha v \beta 3$  integrin and AKT signaling.

### Proteolysis status of NID1 is important to exert its antitumorigenic and immunomodulatory actions

As mentioned, NID1 overexpression mirrored the absence of the protease ADAMTS1<sup>6</sup> (Figure 2 and Supplementary Figure S2). To determine whether NID1 fragments retain

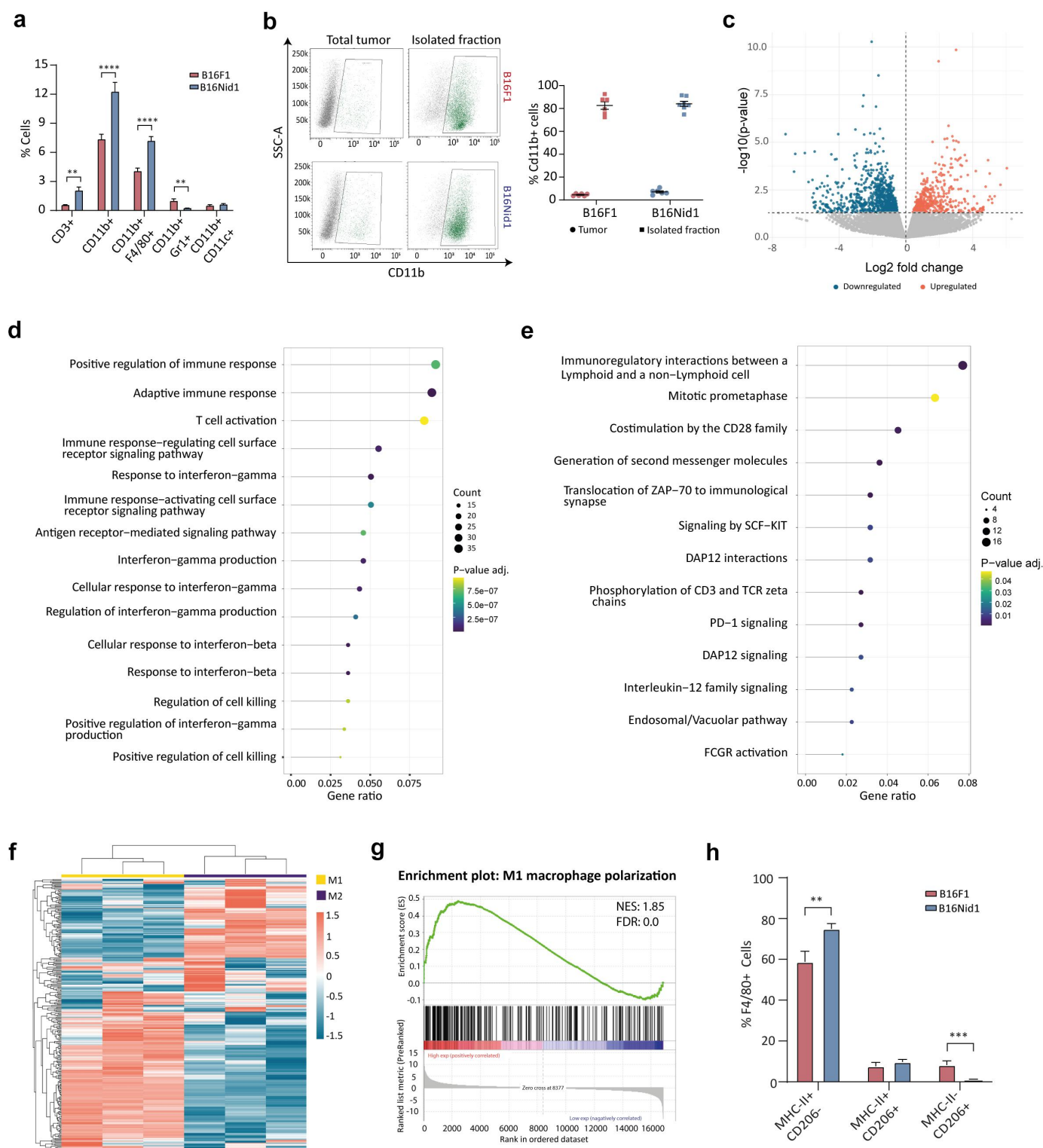


**Figure 3.** Evaluation of immune infiltration in B16Nid1 and B16F1 tumors. (a) Quantification of immune cells in total tumor cell suspensions by FC, including T cells (CD3+), myeloid cells (CD11b+), TAMs (CD11b+ F4/80+), MDSCs (CD11b+/GR1+) and dendritic cells (CD11b+ CD11c+) ( $n \geq 8$  per group). (b) FC plots and quantification of CD11b+ cells in tumors and in the magnetically enriched CD11b+ fraction ( $n = 6$  per group). (c) Volcano plot showing DEGs in CD11b+ cells isolated from B16Nid1 versus B16F1 tumors ( $n = 3$  per group). (d) Top 15 significantly enriched GO biological processes in B16Nid1-derived CD11b+ cells. (e) Significantly enriched pathways identified by Reactome analyses in B16Nid1-derived CD11b+ cells. (f) Heatmap showing up-regulated genes in B16Nid1-derived CD11b+ cells, mapped to M1/M2 macrophage transcriptomic signatures. (g) GSEA of M1-associated genes in B16Nid1 versus B16F1 CD11b+ cells; normalized enrichment score (NES) and statistically significant false discovery rate (FDR) are indicated. (h) FC analysis of the polarization state of TAMs (CD11b+ F4/80+), based on MHC-II (M1 marker) and CD206 (M2 marker) expression ( $n > 10$  per group). (\* $p < 0.05$ ; \*\* $p < 0.01$ ; \*\*\* $p < 0.001$ ).

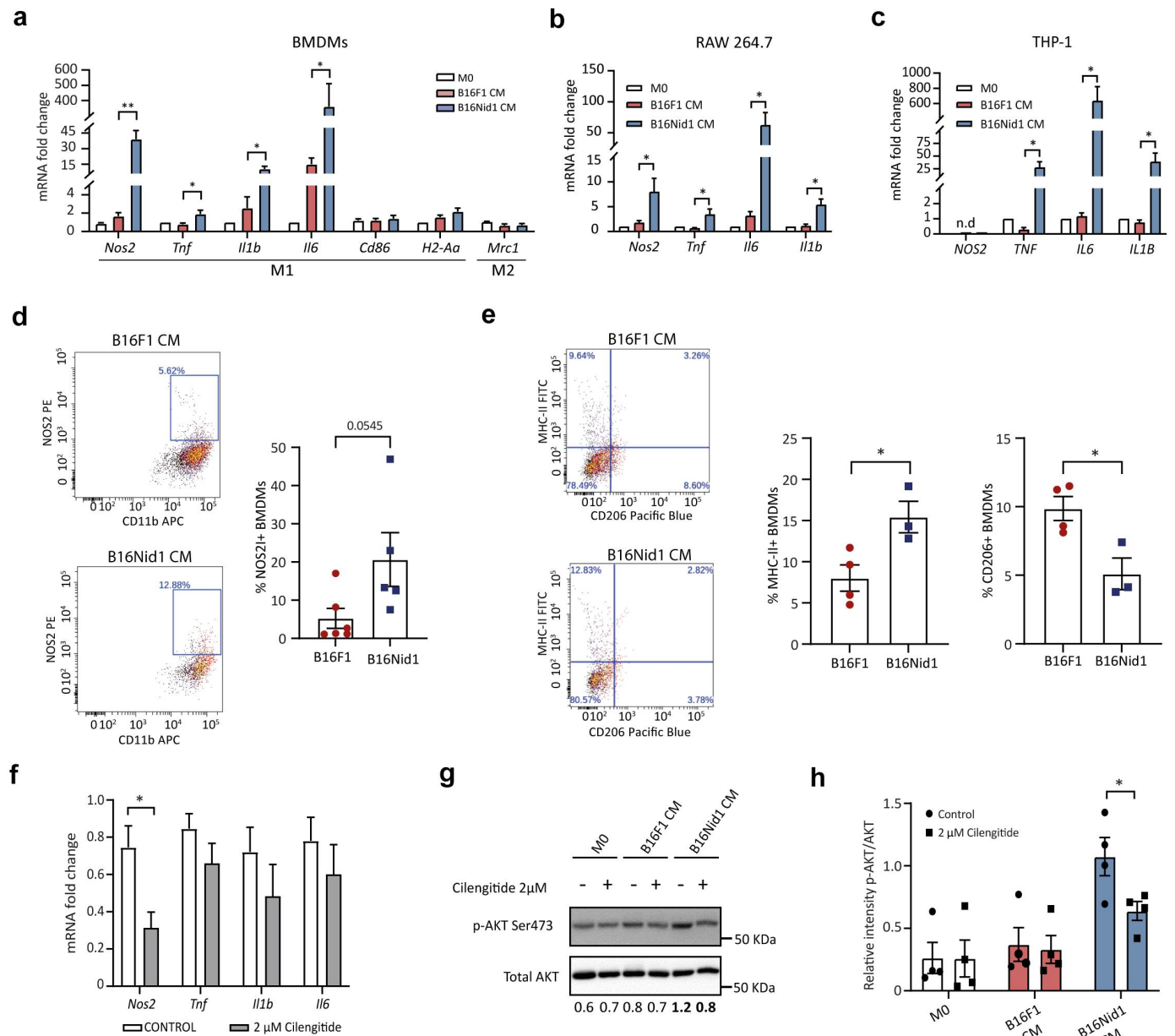


**Figure 4.** *In vitro* macrophage polarization by control and NID1 overexpressing cells. (a) Relative mRNA Fold change expression of M1 (*Nos2*, *Tnf*, *Il1b*, *Il6*, *Cd86* and *H2-Aa*) and M2 (*Mrc1*) polarization-related genes in BMDMs treated with M0 control media, or CM from B16F1 or B16Nid1 cells ( $n = 6$  per group). (b-c) Relative mRNA Fold change expression of M1-related genes in RAW 264.7 cells (b) ( $n = 3$ ) or THP-1-derived macrophages (c) ( $n = 2$ ) treated as in (a). (d-e) FC plots showing NOS2 (d), MHC-II (e) and CD206 (e) expression levels in BMDMs treated with CM from B16F1 and B16Nid1 cells, along with graph representation of their quantification. (f) Relative mRNA Fold change expression of M1-related genes (*Nos2*, *Tnf*, *Il1b*, and *Il6*) in BMDMs polarized with B16Nid1 CM, control or pre-treated with 2  $\mu$ M cilengitide ( $n = 6$  per group). (g) p-AKT and total AKT western blot (WB) analysis of lysates from BMDMs treated during 15 min with M0 control media, or CM from B16F1 or B16Nid1 cells. When indicated, cells were pre-treated with 2  $\mu$ M cilengitide. Digits below each lane correspond to the relative intensity of p-AKT/AKT ratio. (h) Graph representing quantification of p-AKT WB levels normalized to total AKT for each condition ( $n = 4$ ) (\* $p < 0.05$ ; \*\* $p < 0.01$ ).

antitumorigenic properties, we generated two B16F1-derived cell lines overexpressing the ADAMTS1-cleaved NID1 fragments<sup>7</sup> (designated B16G1 and B16G2G3) (Figure 5a and Supplementary Figure S2A-B). *In vivo* tumor growth assays showed significant tumor blockade only in mice bearing B16Nid1 cells, whereas B16G1 and B16G2G3 tumors progressed as B16F1 controls (Figure 5b-c). Evaluation of tumor immune infiltrates revealed that, similar to B16Nid1, B16G1 and B16G2G3 tumors exhibited increased myeloid infiltration (CD11b+ cells), particularly macrophages (CD11b+ F4/80+ cells), compared to B16F1 controls (Figure 5d). However,

MHC-II induction was exclusive to tumors overexpressing full-length NID1 and absent in those expressing the G1 or G2G3 fragments. CD206 expression in the myeloid compartment remained unchanged across all tumor types (Figure 5e). Interestingly, longitudinal analysis of myeloid infiltration revealed that full-length NID1 not only induced macrophage recruitment but also increased infiltration levels from early (day 14) to late (day 20) tumor growth stages (Supplementary Figure S6A).

An exploratory gene expression analysis of inflammatory-related genes in bulk tumor RNA further confirmed upregulation

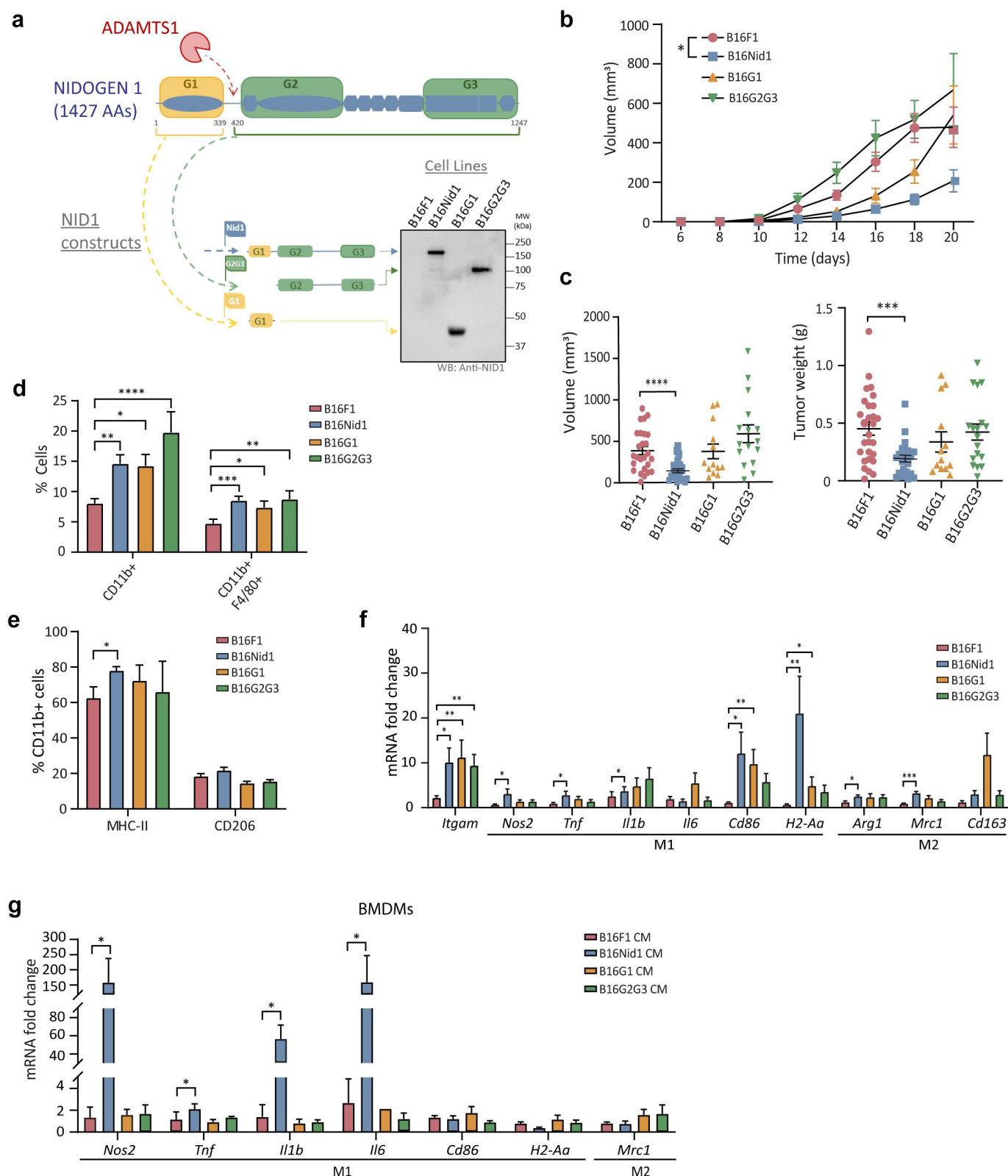


**Figure 5.** Evaluation of tumor progression, immune infiltration and *in vitro* actions of NID1-proteolytic fragments. (a) Scheme showing the protein structure of NID1 and its proteolysis by ADAMTS1. The coding sequence of G1 and G2G3 NID1 fragments is indicated, together with a WB analysis of NID1 forms present in the CM from B16F1, B16Nid1, B16G1 and B16G2G3 cells. Coloured arrows pointed to specific NID1 fragments in each cell line. (b) Evolution of mean tumor volume for each experimental group ( $n \geq 15$  per group). (c) Graphs representing tumor volume and weight at end point for each experimental group. (d) Percentage of myeloid (CD11b<sup>+</sup>) and TAMs (CD11b<sup>+</sup> F4/80<sup>+</sup> cells) in total tumor cell suspensions determined by FC ( $n \geq 14$  per group). (e) Graph representing FC analysis of the polarization markers MHC-II and CD206 in CD11b<sup>+</sup> cells from tumors ( $n \geq 14$  per group). (f) Relative mRNA Fold change of pan macrophage marker: *Itgam*; M1 polarization-related genes: *Nos2*, *Tnf*, *Il1b*, *Il6*, *Cd86* and *H2-Aa*; and M2 polarization-related genes: *Arg1*, *Mrc1* and *Cd163* ( $n \geq 9$  per group). (g) Relative mRNA Fold change expression of M1 (*Nos2*, *Tnf*, *Il1b*, *Il6*, *Cd86* and *H2-Aa*) and M2 (*Mrc1*) polarization-related genes in BMDMs treated with CM from B16F1, B16Nid1, B16G1 or B16G2G3 cells ( $n = 2$ ). (\* $p < 0.05$ ; \*\* $p < 0.01$ ; \*\*\* $p < 0.001$ ; \*\*\*\* $p < 0.0001$ ).



of the pan-myeloid marker *Itgam* in tumors overexpressing both intact and cleaved NID1 (Figure 5f). Although it was performed on bulk tumor, it provides insights into myeloid-lineage activity within the TME. Notably, enhanced expression of M1/pro-inflammatory and M2/anti-inflammatory genes was observed exclusively in B16Nid1 tumors (Figure 5f). To further characterize this response, we estimated a ratio based on *H2-Aa* (MHC-II) and *Mrc1* (Cd206), which was highest in B16Nid1 tumors compared to B16F1, aligning with the FC data (Supplementary Figure S6B).

Finally, *in vitro* BMDM polarization assays revealed that only CM containing intact NID1 induced M1-associated markers expression, whereas NID1 fragments had no such effect (Figure 5g).

Together, these findings indicate that although NID1 proteolytic fragments can recruit myeloid cells, only full-length NID1 is capable of skewing macrophages toward an M1-like phenotype, correlating with its tumor-suppressive activity.

### **Projection of transcriptomic data of NID1-overexpressing tumors reveals a M1-associated gene signature with prognostic value in human melanoma**

The observed NID1-mediated antitumorigenic and immunomodulatory actions *in vivo* and *in vitro* prompted a deeper transcriptomic characterization of our murine model, and their projection onto human melanoma datasets, aiming to identify conserved signatures or biomarkers. Differential expression analysis of bulk RNA-seq data from B16F1 and B16Nid1 tumors revealed 1521 DEGs, with 1009 upregulated and 512 downregulated in the B16Nid1 group (Figure 6a). We then profiled the expression patterns of up-regulated DEGs onto two independent human melanoma cohorts: the Leeds Melanoma Cohort (LMC)<sup>19</sup> and the Skin Cutaneous Melanoma dataset from The Cancer Genome Atlas (SKCM-TCGA) cohort,<sup>20</sup> comprising 703 and 472 melanoma patients respectively. Given the increased immune infiltration observed in B16Nid1 tumors, we designed a bioinformatic pipeline to explore interactions between the identified DEGs and infiltrated immune populations (Figure 6a and Materials and Methods). Successfully, we identify a subset of genes that positive correlated ( $R > 0.4$ ) with M1 macrophage scores in both patient cohorts (Figure 6b–c). The expression pattern of these identified 10 genes, individually or as an “M1-Associated Signature”, grouped patients into high or low expressors across both cohorts (Figure 6d). Very importantly, survival analysis demonstrated that patients with high expression of the “M1-Associated Signature” presented better outcomes in both LMC and SKMC-TCGA datasets (Figure 6e).

These findings highlight the translational relevance of NID1-driven transcriptomic reprogramming in murine melanoma, revealing a gene signature linked to M1-like macrophage abundance that holds prognostic value in human melanoma patients.

### **Discussion**

In recent years, the tumor ECM has emerged as a critical modulator of tumor progression and immune modulation.<sup>1,21</sup> In this study we linked ADAMTS1's pro-tumorigenic actions

to its substrate NID1. Specifically, we reported how elevated NID1 levels induce immune infiltration and inhibit tumor progression, as formerly seen in *Ats1-KO* mice.<sup>6</sup> Additionally, we unveiled a novel immunomodulatory function of NID1 educating macrophages toward an M1-like state. The projection of transcriptomic data from NID1-overexpressing tumors allowed us to discover a new gene signature linked to good prognosis and abundance of M1-like macrophages in melanoma patients.

According to the nature of the glycoprotein NID1, our study evoked previous research underlining the contribution of the BM in cancer.<sup>22,23</sup> However, the specific contribution of nidogens in cancer within this structural context remains unexplored. While various studies have proposed NID1 as a cancer biomarker,<sup>24–27</sup> no functional insights have been provided. Notably, we show that full-length NID1 inhibits tumor progression, whereas proteolyzed forms do not. Increased NID1 deposition around tumor vessels in two distinct *Adamts1*-deficient models suggested that ADAMTS1-mediated proteolysis disrupts NID1's antitumorigenic effect by altering BM structure. Moreover, the observed increase in COL IV with NID1 suggests a more stable vascular BM. Considering ADAMTS1's actions in neovasculture,<sup>4,14</sup> and the key role of vascular endothelium in immune cell trafficking,<sup>28</sup> our data point toward a link between ECM composition, vascular architecture, and immune cell access to the tumor niche.

Emerging knowledge supports a direct role of tumor ECM composition in immunity. Puttock *et al*<sup>29</sup> demonstrated clear links between ECM remodeling and macrophage phenotypes. Although studies connecting NID1 to immune processes are limited, recent research found NID1 in tumor tracks that facilitate immune cell retention in the stroma.<sup>30</sup> Importantly, in our NID1-overexpressing model, NID1 was specifically deposited around blood vessels, potentially aiding immune cell infiltration into tumors. Our results, which show that B16Nid1 tumors maintained or increased immune cell populations over time, support this possibility, although further research is needed for confirmation.

In non-tumoral contexts, early reports described NID1 stimulating neutrophils via its RGD domain,<sup>31</sup> pointing out its integrin-mediated functions. More recently, NID1 has been linked to immune modulation during regeneration,<sup>32</sup> involving  $\alpha\beta3$  integrin. Now our work introduces macrophages as a new immune target of NID1, educating them toward an M1-like inflammatory state.

The role of macrophages in tumoricidal activity and triggering adaptive immune responses is well established. In the B16Nid1 model, NID1 overexpression promotes a transcriptomic reprogramming of the myeloid compartment, characterized by enrichment of IFN signaling, adaptive immune activation, and T-cell activation signatures, all hallmarks of antitumor immunity and consistent with an M1-like, pro-inflammatory phenotype. Supporting this, FC of TAMs showed increased MHC-II expression, critical for antigen presentation and cytotoxic T-cell priming,<sup>33</sup> potentially explaining the higher T-cell infiltration in B16Nid1 tumors. Together with our *in vitro* data, these results suggest that NID1 promotes macrophage polarization toward an antitumorigenic phenotype, contributing to a more immunogenic TME. Further studies are needed to confirm the NID1-



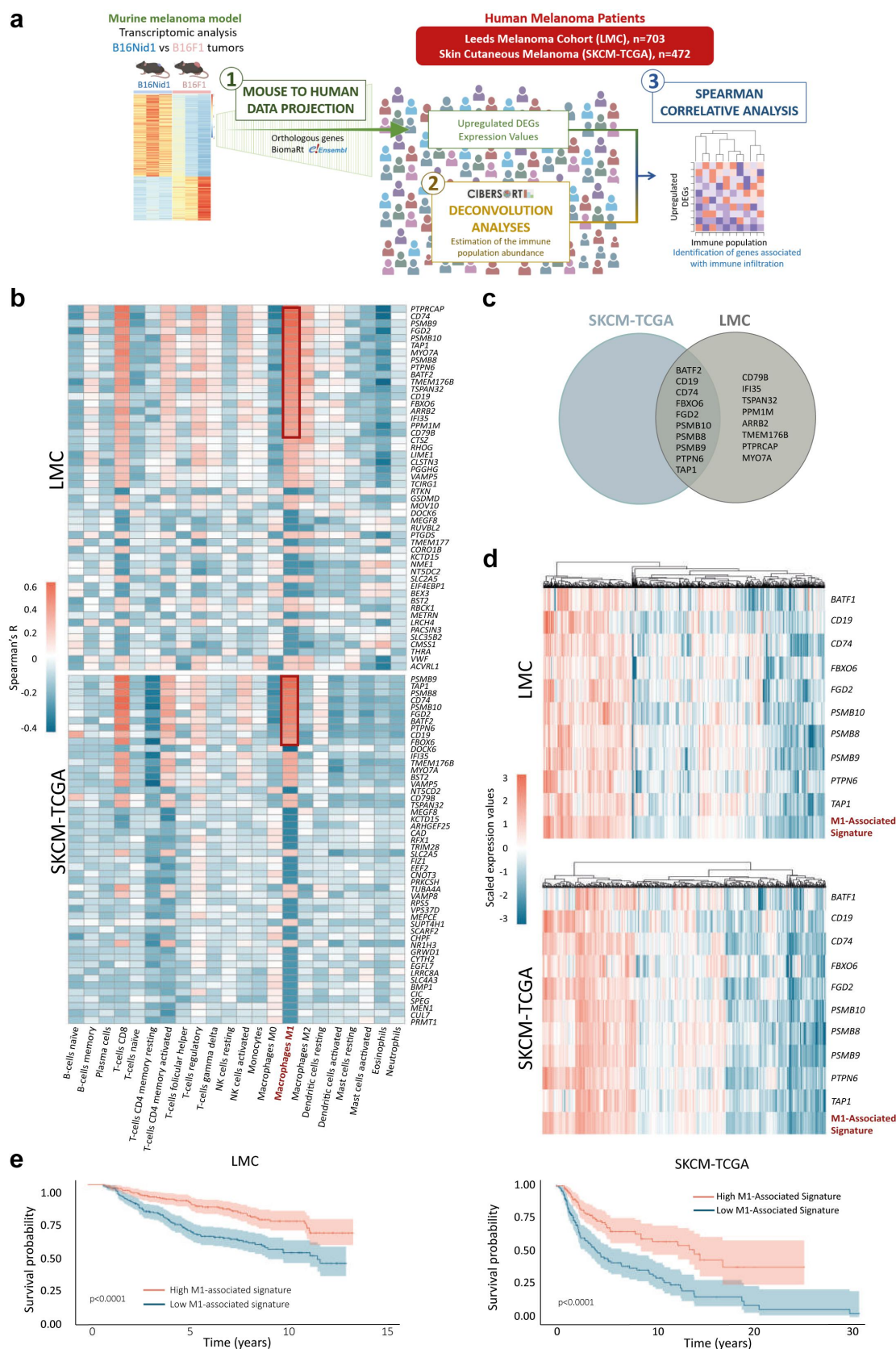


**Figure 6.** Projection of transcriptome mouse data to human melanoma datasets and evaluation as prognosis tool. (a) Scheme of the bioinformatics pipeline used to project transcriptomic data from our mice model to human melanoma patients data, including three main actions: 1: mouse to human data projection, 2: deconvolution analyses of human data, and 3: spearman correlative analysis (more details in material and methods section). (b) Heatmap showing Spearman's *R* values between expression values of up-regulated DEGs and CIBERSORT immune cell scores across LMC and SKCM-TCGA patient cohorts. (c) Venn diagram showing overlap of genes significantly associated with CIBERSORT *M1-associated signature* in LMC and SKCM-TCGA patient cohorts. (d) Heatmap of scaled gene expression values of *M1-associated signature* in LCM and SKCM-TCGA cohorts. (Kaplan-Meier survival curves for 30th percentile of patients expressing high or low levels of *M1-associated signature* in LMC and SKCM-TCGA cohorts.

macrophage-T-cell axis and elucidate the underlying mechanisms.

Driven by the ongoing challenge of deciphering ECM-immune cell interactions,<sup>21</sup> we employed *in silico* approaches to bridge findings from murine to human melanoma. Significantly, our bioinformatic analysis included two large melanoma datasets encompassing over 1100 patients, emphasizing the clinical relevance of the novel “*M1-Associated Signature*” identified from NID1-driven transcriptomic changes. This gene signature, correlated with M1-like macrophage abundance, proved to have strong prognostic value. Among the top identified genes, several -such as CD74, TAP1, and immunoproteasome subunits PSMB8, PSMB9 and PSMB10- are intimately linked to antigen presentation and were all associated with improved survival in melanoma patients.<sup>34,35</sup> Intriguingly, this *M1-Associated Signature* also correlated with predicted enrichment of CD8+ and CD4+ T cells, suggesting a macrophage/T cell interplay within the TME, which likely triggers an immune response against the tumor. This aligns with recent findings describing the existence of a positive activation loop between M1 macrophages and T cells which predicts immunotherapy outcomes across different cancers.<sup>36</sup> Our own observations of increased T cell infiltration in B16Nid1 tumors support further exploration.

Overall, our findings contribute to a deeper understanding of how immune modulation, in our case through ECM remodeling, can improve therapeutic cancer outcomes. Innovative proposals involve developing macrophage-based therapies to sustain their pro-inflammatory and antitumorigenic functions, such as ex-vivo re-polarization and genetic engineering to express proinflammatory transgenes.<sup>37</sup> In this context, our work arises the possibility to engineer macrophages to express full-length NID1. Ultimately, these findings shed new light to understand the intricate extracellular scenario, particularly the intimate relationships between the protease ADAMTS1 and its substrate NID1, stressing the relevance of knowing the distinct roles of intact ECM components and their fragments to improve current therapeutic strategies.

## Acknowledgments

The authors thank JCR-M's laboratory members and GENYO support units for technical assistance and discussions. This manuscript is part of RC-P's Doctoral thesis (Biomedicine Program, UGR, Spain), and benefited from collaborations with COST Actions CA18103, CA20117, and EU-funded CRYSTAL3 (Grant ID 101007931).

## Disclosure statement

No potential conflict of interest was reported by the author(s).

## Funding

The work was supported by the Consejería de Salud y Consumo, Junta de Andalucía [PE-0225-2018]; Ministerio de Ciencia e Innovación, Spain [PID2019-104416RB-I00] Consejería de Universidad, Investigación e Innovación [PROYEXCEL\_00877].

## ORCID

Juan Carlos Rodríguez-Manzanque  <http://orcid.org/0000-0001-5951-7029>

## References

1. Cox TR. The matrix in cancer. *Nat Rev Cancer*. 2021;21(4):217–238. doi: [10.1038/s41568-020-00329-7](https://doi.org/10.1038/s41568-020-00329-7).
2. Winkler J, Abisoye-Ogunniyan A, Metcalf KJ, Werb Z. Concepts of extracellular matrix remodelling in tumour progression and metastasis. *Nat Commun*. 2020;11(1):5120. doi: [10.1038/s41467-020-18794-x](https://doi.org/10.1038/s41467-020-18794-x).
3. Ricard-Blum S, Vallet SD. Fragments generated upon extracellular matrix remodeling: biological regulators and potential drugs. *Matrix Biol: J Int Soc Matrix Biol*. 2019;75–76:170–189. doi: [10.1016/j.matbio.2017.11.005](https://doi.org/10.1016/j.matbio.2017.11.005).
4. Rodríguez-Manzanque JC, Fernández-Rodríguez R, Rodríguez-Baena FJ, Iruela-Arispe ML. ADAMTS proteases in vascular biology. *Matrix Biol: J Int Soc Matrix Biol*. 2015;44–46:38–45. doi: [10.1016/j.matbio.2015.02.004](https://doi.org/10.1016/j.matbio.2015.02.004).
5. Cal S, López-Otín C. ADAMTS proteases and cancer. *Matrix Biol: J Int Soc Matrix Biol*. 2015;44–46:77–85. doi: [10.1016/j.matbio.2015.01.013](https://doi.org/10.1016/j.matbio.2015.01.013).
6. Rodríguez-Baena FJ, Redondo-García S, Peris-Torres C, Martino-Echarri E, Fernández-Rodríguez R, Plaza-Calonge MDC, Anderson P, Rodríguez-Manzanque JC. ADAMTS1 protease is required for a balanced immune cell repertoire and tumour inflammatory response. *Sci Rep*. 2018;8(1):13103. doi: [10.1038/s41598-018-31288-7](https://doi.org/10.1038/s41598-018-31288-7).
7. Canals F, Colomé N, Ferrer C, Plaza-Calonge MDC, Rodríguez-Manzanque JC. Identification of substrates of the extracellular protease ADAMTS1 by DIGE proteomic analysis. *Proteomics*. 2006;6 Suppl 6(S1):S28–35. doi: [10.1002/pmic.200500446](https://doi.org/10.1002/pmic.200500446).
8. Dong L-J, Hsieh J-C, Chung AE. Two distinct cell attachment sites in Entactin are revealed by amino acid substitutions and deletion of the RGD sequence in the cysteine-rich epidermal growth factor repeat 2. *J Biol Chem*. 1995;270(26):15838–15843. doi: [10.1074/jbc.270.26.15838](https://doi.org/10.1074/jbc.270.26.15838).
9. Ma RY, Black A, Qian BZ. Macrophage diversity in cancer revisited in the era of single-cell omics. *Trends Immunol Elsevier Curr Trends*. 2022;43(7):546–563. doi: [10.1016/j.it.2022.04.008](https://doi.org/10.1016/j.it.2022.04.008).
10. Pittet MJ, Michielin O, Migliorini D. Clinical relevance of tumour-associated macrophages. *Nat Rev Clin Oncol* 2022 196. 2022;19(6):402–421. doi: [10.1038/s41571-022-00620-6](https://doi.org/10.1038/s41571-022-00620-6).
11. Mills CD, Kincaid K, Alt JM, Heilman MJ, Hill AM. M-1/M-2 macrophages and the Th1/Th2 paradigm. *J Immunol*. 2000;164(12):6166–6173. doi: [10.4049/jimmunol.164.12.6166](https://doi.org/10.4049/jimmunol.164.12.6166).
12. Parikh R, Parikh S, Berzin D, Vaknine H, Ovadia S, Likonen D, Greenberger S, Scope A, Elgavish S, Nevo Y, et al. Recycled melanoma-secreted melanosomes regulate tumor-associated macrophage diversification. *EMBO J*. 2024;43(17):3553–3586. doi: [10.1038/s44318-024-00103-7](https://doi.org/10.1038/s44318-024-00103-7).
13. Toledo B, Zhu Chen L, Paniagua-Sancho M, Marchal JA, Perán M, Giovannetti E. Deciphering the performance of macrophages in tumour microenvironment: a call for precision immunotherapy. *J Hematol & Oncol*. 2024;17(1):44. doi: [10.1186/s13045-024-01559-0](https://doi.org/10.1186/s13045-024-01559-0).
14. Fernández-Rodríguez R, Rodríguez-Baena FJ, Martino-Echarri E, Peris-Torres C, Del Carmen Plaza-Calonge M, Rodríguez-Manzanque JC. Stroma-derived but not tumor ADAMTS1 is a main driver of tumor growth and metastasis. *Oncotarget*. 2016;7(23):34507–34519. doi: [10.18632/oncotarget.8922](https://doi.org/10.18632/oncotarget.8922).
15. Ricciardelli C, Frewin KM, Tan IDA, Williams ED, Opekin K, Pritchard MA, Ingman WV, Russell DL. The ADAMTS1 protease gene is required for mammary tumor growth and metastasis. *Am J Pathol*. 2011;179(6):3075–3085. doi: [10.1016/j.ajpath.2011.08.021](https://doi.org/10.1016/j.ajpath.2011.08.021).
16. Martino-Echarri E, Fernández-Rodríguez R, Rodríguez-Baena FJ, Barrientos-Durán A, Torres-Collado AX, Del Carmen Plaza-Calonge M, Amador-Cubero S, Cortés J, Reynolds LE, Hodivala-

- Dilke KM, et al. Contribution of ADAMTS1 as a tumor suppressor gene in human breast carcinoma. Linking its tumor inhibitory properties to its proteolytic activity on nidogen-1 and nidogen-2. *Int J Cancer*. 2013;133(10):2315–2324. doi: [10.1002/ijc.28271](#).
17. Chen B, Khodadoust MS, Liu CL, Newman AM, Alizadeh, AA. Profiling tumor infiltrating immune cells with CIBERSORT. *Methods Mol Biol*. 2018;1711:243–259.
  18. Vergadi E, Ieronymaki E, Lyroni K, Vaporidi K, Tsatsanis C. Akt signaling pathway in macrophage activation and M1/M2 polarization. *J Immunol*. 2017;198(3):1006–1014. doi: [10.4049/jimmunol.1601515](#).
  19. Thakur R, Laye JP, Lauss M, Diaz JMS, O'Shea SJ, Poźniak J, Filia A, Harland M, Gascoyne J, Randerson-Moor JA, et al. Transcriptomic analysis reveals prognostic molecular signatures of stage I melanoma. *Clin Cancer Res*. 2019;25(24):7424–7435. doi: [10.1158/1078-0432.CCR-18-3659](#).
  20. Akbani R, Akdemir KC, Aksoy BA, Albert M, Ally A, Amin S, Arachchi H, Arora A, Auman J, Ayala B, et al. Genomic classification of cutaneous melanoma. *Cell*. 2015;161(7):1681–1696. doi: [10.1016/j.cell.2015.05.044](#).
  21. Sutherland TE, Dyer DP, Allen JE. The extracellular matrix and the immune system: a mutually dependent relationship. *Science*. 2023;379(6633):eabp8964. (80–. doi: [10.1126/science.abp8964](#).
  22. Baluk P, Morikawa S, Haskell A, Mancuso M, McDonald DM. Abnormalities of basement membrane on blood vessels and endothelial sprouts in tumors. *Am J Pathol*. 2003;163(5):1801–1815. doi: [10.1016/S0002-9440\(10\)63540-7](#).
  23. Reuten R, Zendejrou S, Nicolau M, Fleischhauer L, Laitala A, Kiderlen S, Nikodemus D, Wullkopf L, Nielsen SR, McNeilly S, et al. Basement membrane stiffness determines metastases formation. *Nat Mater*. 2021;20(6):892–903. doi: [10.1038/s41563-020-00894-0](#).
  24. Ulazzi L, Sabbioni S, Miotto E, Veronese A, Angusti A, Gafà R, Manfredini S, Farinati F, Sasaki T, Lanza G, et al. Nidogen 1 and 2 gene promoters are aberrantly methylated in human gastrointestinal cancer. *Mol Cancer*. 2007;6(1):17. doi: [10.1186/1476-4598-6-17](#).
  25. Li L, Zhang Y, Li N, Feng L, Yao H, Zhang R, Li B, Li X, Han N, Gao Y, et al. Nidogen-1: a candidate biomarker for ovarian serous cancer. *Jpn J Clin Oncol*. 2015;45(2):176–182. doi: [10.1093/jjco/hyu187](#).
  26. Willumsen N, Bager CL, Leeming DJ, Bay-Jensen A-C, Karsdal MA. Nidogen-1 degraded by Cathepsin S can be quantified in serum and is associated with non-small cell lung cancer. *Neoplasia (U States)*. 2017;19(4):271–278. doi: [10.1016/j.neo.2017.01.008](#).
  27. Ko CJ, Huang CC, Lin HY, Juan C-P, Lan S-W, Shyu H-Y, Wu S-R, Hsiao P-W, Huang H-P, Shun C-T, et al. Androgen-induced TMPRSS2 activates matriptase and promotes extracellular matrix degradation, prostate cancer cell invasion, tumor growth, and metastasis. *Cancer Res*. 2015;75(14):2949–2960. doi: [10.1158/0008-5472.CAN-14-3297](#).
  28. Amersfoort J, Eelen G, Carmeliet P. Immunomodulation by endothelial cells — partnering up with the immune system? *Nat Rev Immunol*. 2022 229. 2022;22(9):576–588. doi: [10.1038/s41577-022-00694-4](#).
  29. Puttock EH, Tyler EJ, Manni M, Maniati E, Butterworth C, Burger Ramos M, Peerani E, Hirani P, Gauthier V, Liu Y, et al. Extracellular matrix educates an immunoregulatory tumor macrophage phenotype found in ovarian cancer metastasis. *Nat Commun*. 2023;14(1):2514. doi: [10.1038/s41467-023-38093-5](#).
  30. Fonta CM, Loustau T, Li C, Poilil Surendran S, Hansen U, Murdamoothoo D, Benn MC, Velazquez-Quesada I, Carapito R, Orend G, et al. Infiltrating CD8+ T cells and M2 macrophages are retained in tumor matrix tracks enriched in low tension fibronectin fibers. *Matrix Biol : J Int Soc for Matrix Biol*. 2023;116:1–27. doi: [10.1016/j.matbio.2023.01.002](#).
  31. Senior RM, Gresham HD, Griffin GL, Brown EJ, Chung AE. Entactin stimulates neutrophil adhesion and chemotaxis through interactions between its arg-gly-asp (RGD) domain and the leukocyte response integrin. *J Clin Invest*. 1992;90(6):2251–2257. doi: [10.1172/JCI116111](#).
  32. Zbinden A, Layland SL, Urbanczyk M, Carvajal Berrio DA, Marzi J, Zauner M, Hammerschmidt A, Brauchle EM, Sudrow K, Fink S, et al. Nidogen-1 mitigates ischemia and promotes tissue survival and regeneration. *Advancement Sci*. 2021;8(4):2002500. doi: [10.1002/adv.202002500](#).
  33. Abelin JG, Harjanto D, Malloy M, Suri P, Colson T, Goulding SP, Creech AL, Serrano LR, Nasir G, Nasrullah Y, et al. Defining HLA-II ligand processing and binding rules with Mass spectrometry enhances cancer epitope prediction. *Immunity*. 2019;51(4):766–779.e17. doi: [10.1016/j.immuni.2019.08.012](#).
  34. Kalaora S, Lee JS, Barnea E, Levy R, Greenberg P, Alon M, Yagel G, Bar Eli G, Oren R, Peri A, et al. Immunoproteasome expression is associated with better prognosis and response to checkpoint therapies in melanoma. *Nat Commun*. 2020 111. 2020;11(1):1–12. doi: [10.1038/s41467-020-14639-9](#).
  35. Pérez-Guijarro E, Yang HH, Araya RE, El Meskini R, Michael HT, Vodnala SK, Marie KL, Smith C, Chin S, Lam KC, et al. Multimodel preclinical platform predicts clinical response of melanoma to immunotherapy. *Nat Med*. 2020;26(5):781–791. doi: [10.1038/s41591-020-0818-3](#).
  36. Yang J, Liu Q, Shyr Y. A large-scale Meta-analysis reveals positive feedback between macrophages and T cells that sensitizes tumors to immunotherapy. *Cancer Res*. 2024;84(4):626–638. doi: [10.1158/0008-5472.CAN-23-2006](#).
  37. Sloas C, Gill S, Klichinsky M. Engineered CAR-Macrophages as adoptive immunotherapies for solid tumors. *Front Immunol*. 2021;12:783305. doi: [10.3389/fimmu.2021.783305](#).